Journal of Alloys and Compounds 499 (2010) 273–277

Contents lists available at ScienceDirect

Journal of Alloys and Compounds

journal homepage: www.elsevier.com/locate/jallcom

Effect of differential speed rolling on the anisotropy of mechanical properties and texture evolution of AZ31 Mg alloys

J.B. Lee [a,*], T.J. Konno [a], H.G. Jeong [b]

[a] Institute for Materials Research, Tohoku University, 2-1-1 Katahira, Aoba-ku, Sendai 980-8577, Japan
[b] Advanced Materials Division, Advanced Functional Material Team, Korea Institute of Industrial Technology, 994-32, Dongchon-dong, Yeonsu-gu, 463-130 Incheon, Republic of Korea

ARTICLE INFO

Article history:
Received 29 January 2009
Accepted 22 March 2010
Available online 27 March 2010

Keywords:
Metals and alloys
Mechanical properties
Transmission electron microscopy
TEM

ABSTRACT

We herein report a significant improvement of the ductility of AZ31 (Al: 3 wt%, Zn: 1 wt%, balance Mg) sheets processed by differential speed rolling (DSR). The DSR sheets under tension in the rolling direction exhibited a plastic strain more than 1.5 times larger than the sheets prepared by conventional rolling (CR), and simultaneous improvements of in-plane isotropy. The origin of these changes has been examined by texture and structural characterizations. The (0 0 0 2) pole intensity of the as-rolled DSR sheet is strongly accumulated in the normal direction, which is preserved after deformation regardless of tensile directions; while that of as-rolled CR sheet show clear splitting, which further broadens after tensile tests. It is suggested that these changes are brought about by the application of a large shear strain to DSR sheets, which resulted in the clear (0 0 0 2) texture, and subsequent ease of the activation of prismatic slip during the deformation.

1. Introduction

From the engineering points of view, magnesium alloys are of growing interest because of their potential as a structural material with a large strength-to-weight ratio. For example, in the transportation industry, utilization of Mg alloys for vehicles improves fuel efficiency through their light weight [1], while Mg alloys are being used in the IT industry as a body material personal computer, etc. However up to present, the application of Mg alloys to industry has been limited due to their poor deformability [2,3] and the die-casting is the principle mean for shaping [4]. In particular, improving their ductility has been the subject of much research [5,6], and a number of investigations on the use of Mg alloys sheets have been conducted in search of an optimal processing condition [7]. In case of extrusion of Mg alloys, for example, it has been reported that equal channel angular pressing (ECAP) process takes advantage of a high strain rate more than conventional extrusion, improving the ductility of the Mg alloys. Severe plastic deformations (SPD) by ECAP process can be achieved by refining grain size accompanied with texture evolution, which ultimately leads to the enhancement of mechanical properties [8–11]. Among the techniques studied for sheet production at a large scale, the differential speed rolling (DSR) process is considered promising, and has been known to produce Mg alloy sheets having fine grains [12]. It is also known that it leads to the preferential (0 0 0 2) texture, as in the case of ECAP [13]. It has been proposed that these changes are due to the fact that the DSR process induces stronger shear stress within the sheet than the conventional rolling (CR) process does, due to a large speed difference between the two rollers. Although a considerable amount of phenomenological information on the DSR of Mg alloy sheets has been accumulated in recent years [12–14], our understanding of the microstructure and texture evolution during the process is still inadequate in order to make possible the reliable fabrication of Mg-based products. In addition, the mechanical property of the Mg sheets processed by DSR is not well known. The purpose of this work, therefore, was to examine the effects of DSR on the improvement of their mechanical properties, and elucidate the underlying mechanisms from the viewpoints of microstructure and the texture evolution.

2. Experimental

Commercial AZ31B (Mg–3 wt%Al–1 wt%Zn–0.3 wt%Mn) sheets, 2 mm thick, were employed as starting materials. Prior examinations by optical microscopy (OM) showed that all specimens had equiaxial grains of approximately 50 μm. CR sheets were produced by rolling them at the rolling speed of 0.67 mm/min for the rollers. For DSR sheets, the rolling speeds of the upper and lower rollers were 2 mm/min and 0.67 mm/min, respectively. The temperature of the roller was maintained at 423 K for the both processes. After preheating the specimens at 423 K for 5 min, they were rolled at a reduction rate of 15% by 1 pass without lubrication. To investigate the anisotropy of tensile properties, we prepared tensile specimens by cutting the rolled sheets at 0°, 45°, and 90° from the rolling direction and machined them to a gage having dimension of 25 mm long, 10 mm wide, 1.7 thick. These angles will be referred to as tensile axis (TA) directions. The tensile tests were then conducted at a strain rate of 1×10^{-1} s^{-1} at room temperature using a (MTS810) tensile

* Corresponding author. Tel.: +81 22 215 2126; fax: +81 22 215 2126.
E-mail addresses: jblee@imr.tohoku.ac.jp, verkam7@naver.com (J.B. Lee).

0925-8388/$ – see front matter © 2010 Elsevier B.V. All rights reserved.
doi:10.1016/j.jallcom.2010.03.186

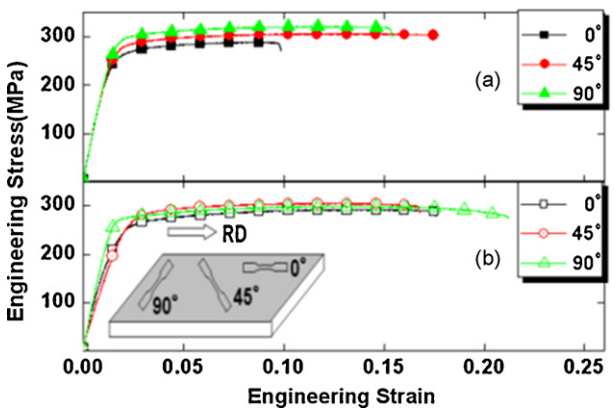

Fig. 1. Engineering stress–strain curves of (a) CR and (b) DSR sheets at room temperature.

tester. Specimens for OM observations were prepared by polishing the normal sections (ND plane) of the rolled sheets and by successive etching in a solution of picric and acetic acids. TEM specimens were prepared after tensile deformation by conventional electro-polishing and ion-thinning methods. We employed JEOL 2000FX operating at 200 kV for TEM observation. In order to measure texture evolution, two pole figures, (0 0 0 2) and $1\,0\,\bar{1}\,1$ for each set of specimens were obtained by using an X-ray diffraction goniometer in the back reflection mode with Cu-K_α radiation, covering an angular region of up to 70° using the Schultz reflection method.

3. Results

Fig. 1 shows the stress–strain curves, measured at room temperature, of (a) CR and (b) DSR sheets. As seen, the plastic strains of the DSR sheets are generally larger than those of CR sheets, especially those with TA = 0° and 90°. It is also evident that the variation among the curves tested in the three different tensile directions is much reduced in the case of DSR. For example, the yield stresses (YS) of the CR sheets were observed to increase with the increase of tensile angle from RD, but this tendency is less pronounced in the case of DSR. Also the ultimate tensile strengths (UTS) of DSR, which is generally larger than that of CR, are near 300 MPa for all tensile angles, exhibiting orientational isotropy.

Fig. 2 shows the microstructure, as observed by OM, in the mid-plane of (a) CR and (b) DSR sheets obtained with a reduction rate of 15% before tensile tests. As seen, the rolled sheets consist of grains of 10–40 μm, often displaying stripe contrasts, which is suggestive of the presence of twins.

Fig. 3 shows, respectively, (0 0 0 2) and $1\,0\,\bar{1}\,1$ pole figures of the same set of the specimens. It can be observed that the (0 0 0 2) pole of the CR sheet splits into two peaks by about 5° in RD, while that of DSR sheet does not but inclined about 7° toward the RD. In fact the intensity of the (0 0 0 2) peak of the latter is 1.5 times as large as that of the CR sheet, as indicated in the figures. Correspondingly, the $1\,0\,\bar{1}\,1$ poles of the CR sheets exhibit only weak accumulation about transverse direction (TD), while those of DSR shows intense semicircular distribution. These observations suggest that the DSR sheet possess a texture circularly more uniform about ND than that of CR sheets.

Fig. 4 shows the microstructure of the mid-plane of fractured specimens after the tensile tests, as observed by OM. Here, the rolling and tensile directions are indicated in the figure. For the CR samples ((a)–(c)), the fractured specimens consist of grains of 10–30 μm with relatively homogeneous size distribution. The presence of a number of stripe contrasts within the grains is evident. In contrast, the size distribution of grains in the DSR sample is rather heterogeneous: colonies of fine grains and coarse grains co-exist within the sheets, and often stripe contrasts are seen to traverse from one grain to the other. Note also that these stripe contrasts, which are due to twin generally appear along the direction perpendicular to the tensile direction in both cases where TA = 90° ((c) and (f)). This tendency is less pronounced as the TA direction decreases and becomes parallel to RD ((a) and (d)).

Fig. 5 shows (0 0 0 2) pole figures obtained from the mid-planes of fractured CR and DSR sheets, as a function of tensile angles. For CR sheets, the peak intensities of (0 0 0 2) poles become weaker, i.e., from 9.6 to about 6–7, and it can be seen that the strong intensities distribute in the tensile direction. For DSR sheets, in contrast, the spread of the pole is smaller than that of the CR sheets resulting in strong peak intensities, despite the fact that these specimens had exhibited a larger tensile strain before fracture. Moreover, a closer observation reveals that the poles spread perpendicular to the tensile direction, unlike in the case of CR.

Fig. 6 shows $1\,0\,\bar{1}\,1$ pole figures of the same set of the specimens as a function of tension directions. The poles of the CR samples show concentric distribution with slight increase of the intensities perpendicular to the tensile direction. On the other hand, those in DSR samples show a clear systematic 6-fold intensity variation. Furthermore, as seen, there is very little dependence on the orientation of the tension. In particular, it should be pointed out that the pole figures of the DSR samples that underwent the tensile tests at 0°, 45°, and 90° from RD exhibit qualitatively identical hexagonally symmetric distribution of the $1\,0\,\bar{1}\,1$ poles.

Fig. 7 shows TEM bright field micrographs of a mid-plane of fractured DSR tensile specimen. The TEM bright field image of the specimen was taken with the incident electron beam along the $1\,1\,\bar{2}\,0$ axis under the two-beam diffraction condition with $g = \bar{1}\,1\,0\,1$, in order to image all distortions perpendicular to the *a*-axis. In this figure, a number of dark contrasts arise from strain fields around dislocations. As seen, these contrasts are mostly lie on the (0 0 0 2) planes, but occasionally we found contrasts perpendicular to the basal plan. For example, the short white arrow in

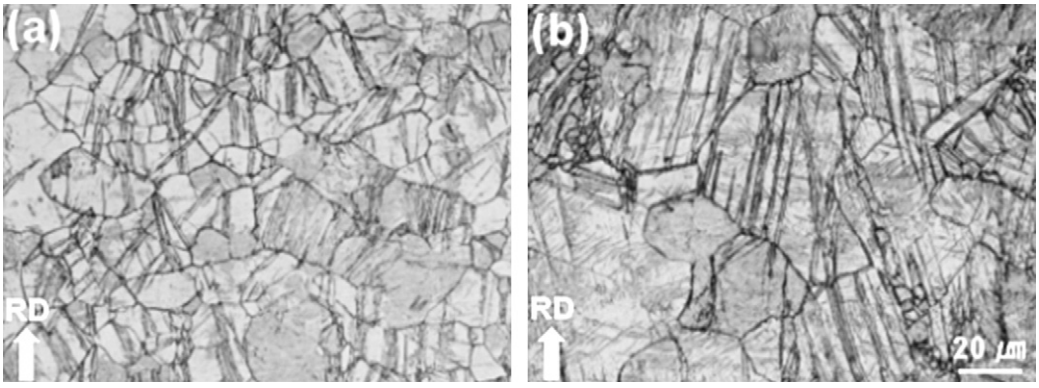

Fig. 2. Micrographs of (a) CR and (b) DSR sheet before deformation.

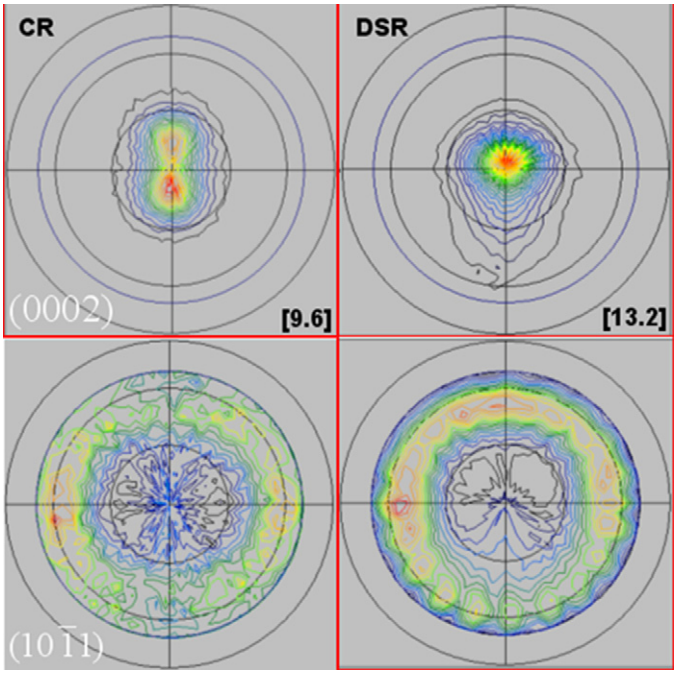

Fig. 3. (0002) pole figures (upper) and (1 0 $\bar{1}$ 1) pole figure (lower) of CR (left) and DSR (light) samples rolled at 423 K with reduction rate of 15%. Mid-plane of all the samples was examined. The number in brackets indicates the peak intensity of the (0002) pole figures.

Fig. 7(b) indicates the dislocation whose slip planes changed from the basal to the prismatic plane.

4. Discussion

In this study, we showed that the mechanical properties of the AZ31 alloy improved considerably by DSR in all tensile directions, i.e., TA = 0°, 45° and 90°. It was also shown that the angular variations of the mechanical properties, in terms of both YS and UTS with respect to the rolling direction, are much reduced by DSR, exhibiting the angular homogeneity of the DSR sheets. Correspondingly, the evolution of texture and microstructure in these two kinds of sheets were found to be fundamentally different. These observations, in particular the texture evolution, indicate that the operating mode for the deformation of the DSR sheet is different from that of CR.

In terms of the texture of as-rolled CR and DSR specimens, the (0002) peak intensity in the CR specimens is split into the rolling direction, while that of the DSR exhibits strong accumulation in the normal direction, ND. This difference demonstrates that grains in the as-rolled CR sheets possess two symmetrically equivalent orientations, while that those of as-rolled DSR possess single, but circularly distributed orientation. The weak double-peak texture of CR samples is recently found in the simulation study by Agnew et al. [15]. They explained that the tendency of the (0002) intensity to split is enhanced primarily by an increase in the activation of <c + a> slip rather than prismatic slip. On the other hand, the reason for the tilted peak texture of DSR samples, as observed in Fig. 3(b) in the present work, was in fact suggested by Couling et al. [16] and Wonsiewiez and Backofen [17]. They showed that secondary {1 0 $\bar{1}$ 2} twinning and basal slip within primary {1 0 $\bar{1}$ 1} compression twins may result in the tilted peak.

From the viewpoints of mechanical properties of these two kinds of sheets, we showed in general that the YS values of both CR and DSR samples increases as the tensile angle from RD increases. Our results, however, suggested that this tendency is less pronounced in the DSR sheets. That the CR samples show slightly higher YS values than DSR samples for RD has partly been explained by several authors [18,19]: DSR samples have more coarse grains than CR samples, an observation also made in the present study (Fig. 2). The larger elongation of DSR samples, particularly when the tensile test is made parallel to RD, cannot be understood however, only on the basis of the grain size difference [19], and indicate that the operating mode for the deformation under tension is significantly different in these two kinds of Mg sheets.

For example, during deformation, we found that the evolution of texture of DSR sheets is significantly different from that of CR sheets. That is, the decrease and broadening of the (0002) peak intensity of the former under tension is small, and in fact it broadened perpendicular to the tensile direction, on the contrary to the observation made for the CR sheets. Correspondingly the 1 0 $\bar{1}$ 1 peak intensity showed qualitatively identical 6-fold distributions,

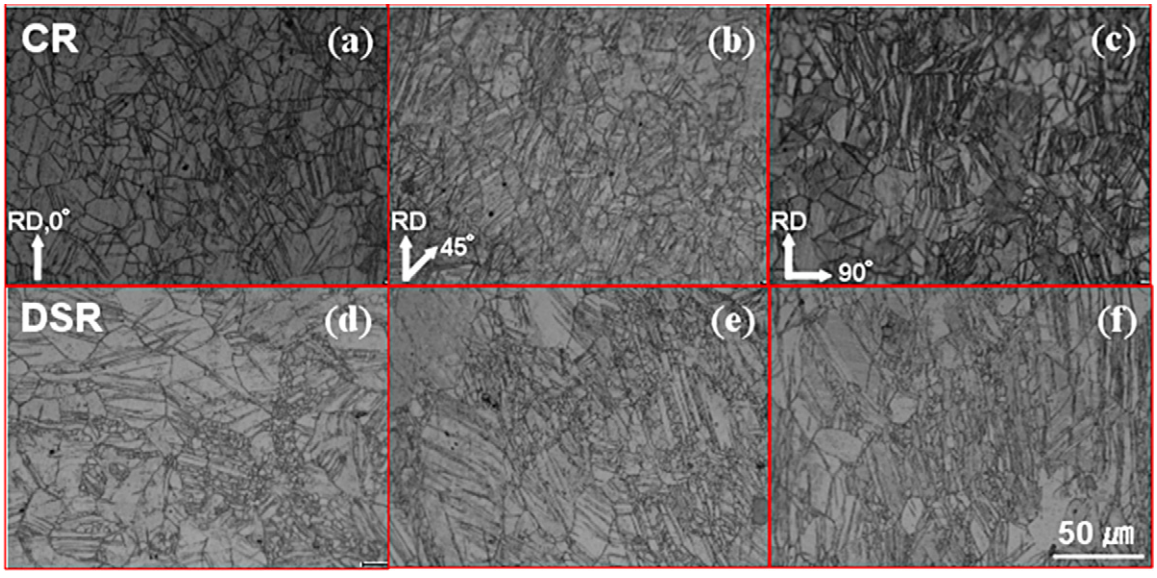

Fig. 4. Micrographs of CR and DSR samples as a function of tension angle from rolling direction (RD) after fracture of tensile test. Many fine grains around coarse grains can be seen in the DSR samples for all tension directions.

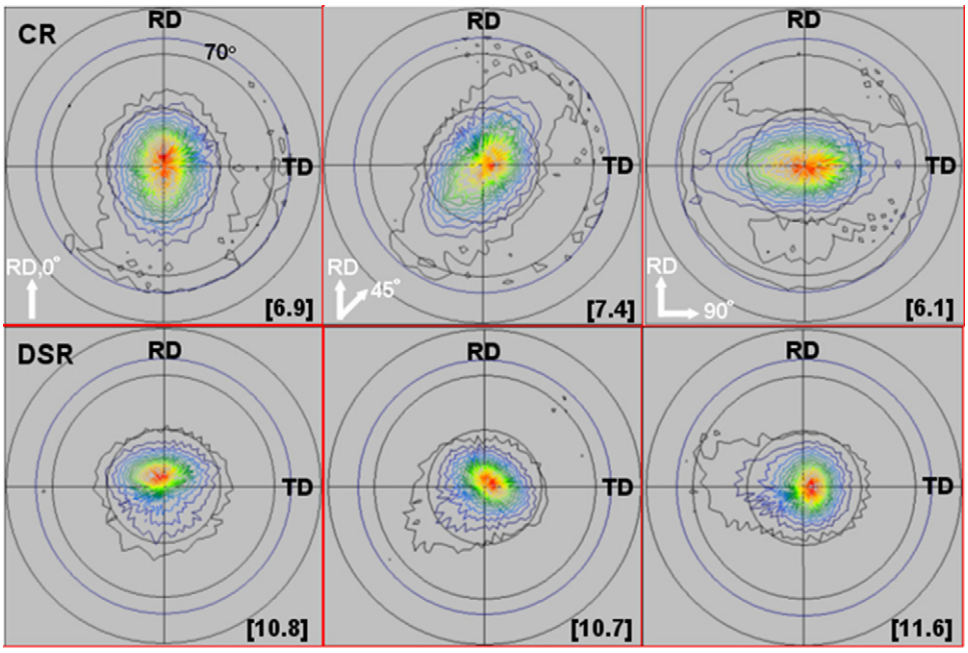

Fig. 5. (0 0 0 2) pole figures of CR (upper) and DSR (lower) samples after fracture as a function of tension angles from rolling direction (RD) after fracture of tensile test. The number in brackets indicates the intensity of the (0 0 0 2) pole figures.

irrespective of the tensile direction, TA, of 0°, 45° or 90°. This behavior is in marked contrast with that of the CR sheets, where the (0 0 0 2) peaks show clear broadening in the RD, which is suggestive of the activation of <c + a> slip.

These observations led us to propose that the deformation modes are different in these alloys. For the CR sheets, a fairly strong hexagonal (0 0 0 2) oriented texture, and the random distribution of $1\,0\,\bar{1}\,1$ poles suggest that the basal slip is the dominant mechanism. For the DSR sheets, on the other hand, the slight inclination of (0 0 0 2) poles and the 6-fold development of $1\,0\,\bar{1}\,1$ poles distribution suggest that, in addition to the basal slip, the prismatic slip must be in operation. It should be pointed out that the $1\,0\,\bar{1}\,1$ pole figures of DSR samples at all tension angles examined in this study exhibited basically identical intensity distribution, irrespective of the tensile direction, TA. This observation strongly suggests that the activation of prismatic slip is responsible for the deformation in the DSR sheets. In addition, Koike and Ohyama, using an AZ61 (Mg–6Al–1Zn in wt%) sheet, showed that the basal plane tilt angle with respect to the tensile direction is an essential geometrical criterion for the activation of the basal or prismatic <a> slip at room temperature [20]. Namely, they concluded that basal <a> slip is dominant when the Mg basal plane is tilted more than 16.5° towards TA, while prismatic <a> slip system become active when the basal plane is less than this angle. Our texture measure-

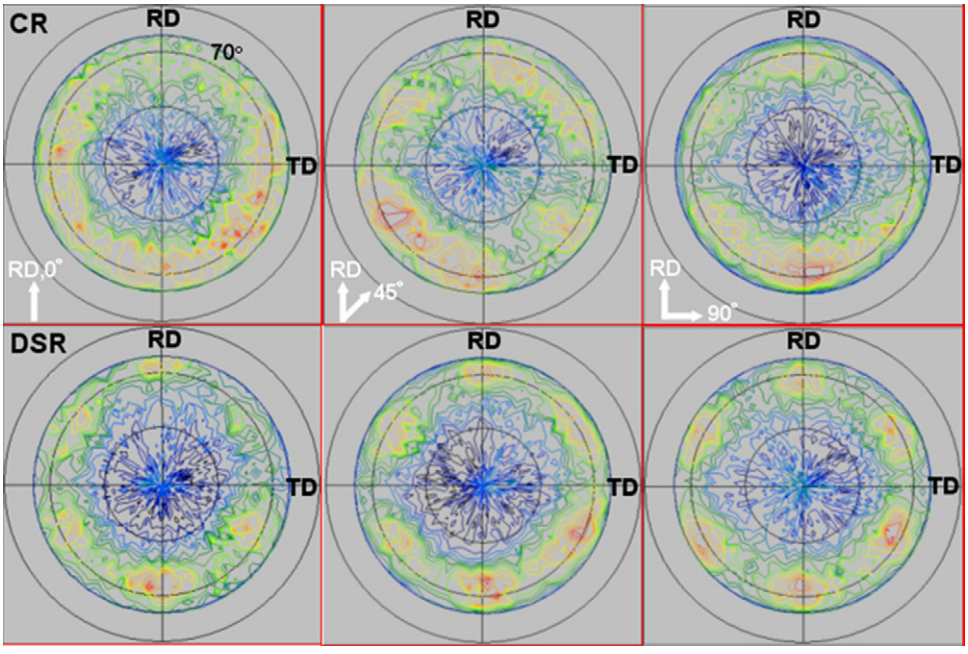

Fig. 6. $(1\,0\,\bar{1}\,1)$ pole figure of CR (upper) and DSR (lower) samples as a function of the tension angles from rolling direction (RD) after the tensile test.

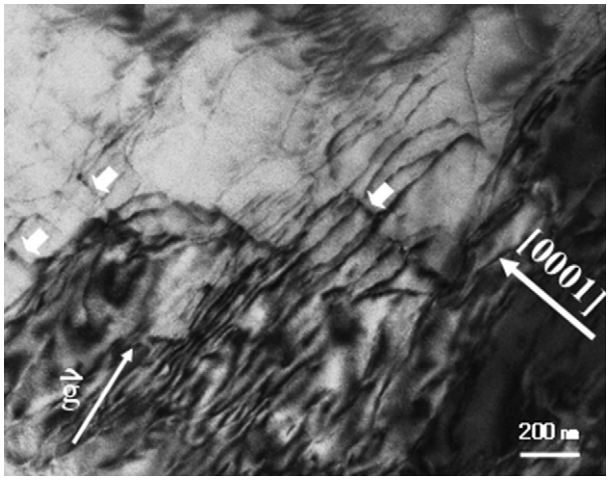

Fig. 7. TEM bright field images of DSR sample with elongation of 18% at room temperature taken along [1 1 $\bar{2}$ 0] with $g = \bar{1}\,1\,0\,1$, which is shown by long arrows. The short white arrow indicates the dislocation slip from basal plane to the prismatic slip.

ments suggested that the basal <a> slip is the major deformation mode in the CR specimen, while the prismatic <a> slip system plays the dominant role in the DSR specimen. In dependently, Our TEM investigation showed a contrast arising from a dislocation line perpendicular to the basal plane, an indication of the activation of a prismatic slip. Thus, it may be concluded that prismatic slips can easily take place in DSR samples than in CR because of the strong accumulation of the *c*-axis along ND. From practical points of view, this observation, in return, indicates that the microstructure and texture of the rolled sheets processed by DSR is effective in making dislocations move easily along the prismatic plane, at a lower stress.

To summarize, we show that the ductility of AZ31B sheets processed by DSR is superior to that prepared by CR. This improvement is due not to the grain size, but primarily to the orientation of the grains. The DSR method, with its large shear stress, is effective in maintaining the *c*-axis parallel to ND, which facilitates prismatic slip, and thereby results in a large elongation.

5. Conclusion

We studied the mechanical properties of AZ31B alloy sheets rolled with DSR and CR processes, by means of tensile tests in the tensile directions 0°, 45°, and 90° from the original RD, and investigated the underlying mechanisms of the observed difference from the viewpoints of texture evolution and structural characterization. The results can be summarized as follows: (1) The *c*-axis of the Mg grains in the as-rolled DSR sheets exhibited strong accumulation in ND, while that of CR showed clear 2-fold distribution tilted towards RD. (2) The elongation of the DSR sheets in all the tensile directions before fracture is larger than that of the CR sheets. (3) After deformation, the texture of the DSR sheets is characterized, regardless of the tensile direction, by the small dispersion of the *c*-axis of the grains and the 6-fold distribution of prismatic planes; while the CR sheets exhibit broad re-distribution of *c*-axis in the tensile direction and corresponding random distribution of prismatic plane orientation. (4) TEM observation of the deformed DSR sheets showed the evidence of prismatic slip. These observations indicate that the DSR sheets maintain a large number of grains with their *c*-axis in ND during tensile deformation, facilitating the activation of the prismatic slip, which in return, resulted in in-plane isotropy of the mechanical property and a large degree of ductility of the DSR sheets.

Acknowledgements

The authors express their sincere thanks to Prof. A. Chiba and Dr. H. Matsumoto of Tohoku University for the provision of the laboratory facility.

References

[1] D. Eliezer, E. Aghion, H. Fores, Proc. First Israeli Int. Conf. Magnesium Sci. Technol., 1977, p. 343.
[2] H. Somekawa, H. Hosokawa, H. Watanabe, Mater. Sci. Eng. A 339 (2003) 328–333.
[3] K. Kitazono, E. Sato, K. Kuribayashi, Scripta Mater. 44 (2001) 2695–2702.
[4] A. Stalmann, W. Sebastian, H. Friedrich, S. Schumann, K. Droder, Adv. Eng. Mater. 3 (2001) 969–974.
[5] S.R. Agnew, J.A. Horton, T.M. Lillo, D.W. Brown, Scripta Mater. 50 (2004) 377–381.
[6] M. Kai, Z. Horita, T.G. Langdon, Mater. Sci. Eng. A 488 (2008) 117–127.
[7] H. Koh, T. Sakai, H. Utsunomiya, S. Minamiguchi, Mater. Trans. 48 (2007) 2023–2027.
[8] M. Mabuchi, K. Ameyama, H. Iwasaki, K. Higashi, Acta Mater. 47 (1999) 2047–2057.
[9] H.K. Lin, J.C. Huang, T.G. Langdon, Mater. Sci. Eng. A 402 (2005) 250–257.
[10] A. Yamashita, Z. Horita, T.G. Langdon, Mater. Sci. Eng. A 300 (2001) 142–147.
[11] W.J. Kim, S.I. Hong, Y.S. Kim, S.H. Min, H.T. Jeong, J.D. Lee, Acta Mater. 51 (2003) 3293–3307.
[12] W.J. Kim, J.B. Lee, W.Y. Kim, H.T. Jeong, H.G. Jeong, Scripta Mater. 56 (2007) 309–312.
[13] H. Watanabe, T. Mukai, K. Ishikawa, J. Mater. Proc. Technol. 182 (2007) 644–647.
[14] W. Xia, Z. Chan, D. Chen, S. Zhu, J. Mater. Proc. Technol. 209 (2009) 26–31.
[15] S.R. Agnew, M.H. Yoo, C.N. Tome, Acta Mater. 49 (2001) 4277–4289.
[16] S.L. Couling, J.F. Pashak, L. Sturkey, Trans. ASM 51 (1959) 94.
[17] B.C. Wonsiewicz, W.A. Backofen, Trans. AIME 239 (1967) 1422.
[18] S.-B. Yi, C.H.J. Davis, H.-G. Brokmeier, R.E. Bolmaro, K.U. Kainer, J. Homeyer, Acta Mater. 54 (2006) 549–562.
[19] M.R. Barnett, S. Jacob, B.F. Gerard, J.G. Mullins, Scripta Mater. 59 (2008) 1035–1038.
[20] J. Koike, R. Ohyama, Acta Mater. 53 (2005) 1963–1972.